

Efficiency Enhancement of Inverted Polymer Solar Cells Using Ionic Liquid-functionalized Carbon Nanoparticles-modified ZnO as Electron Selective Layer

Feng Zhu¹, Xiaohong Chen^{1,*}, Zhe Lu¹, Jiaxiang Yang², Sumei Huang¹, Zhuo Sun¹

(Received 08 September; accepted 18 November 2013; published online 30 December 2013)

Abstract: ZnO thin film was fabricated on tin-doped indium oxide electrode as an electron selective layer of inverted polymer solar cells using magnetron sputtering deposition. Ionic liquid-functionalized carbon nanoparticles (ILCNs) film was further deposited onto ZnO surfaces by drop-casting ILCNs solution to improve interface properties. The power conversion efficiency (PCE) of inverted polymer solar cells (PSCs) with only ZnO layer was quickly decreased from 2.7% to 2.2% when the thickness of ZnO layer was increased from 15 nm to 60 nm. However, the average PCE of inverted PSCs with ZnO layer modified with ILCNs only decreased from 3.5% to 3.4%, which is comparable to that of traditional PSCs with poly(3,4-ethylenedioxythiophene)/poly(styrenesulfonate) anode buffer layer. The results suggested that the contact barrier between ZnO layer and poly(3-hexylthiophene) and phenyl-C₆₁-butyric acid methylester (P3HT:PCBM) blended film compared to ZnO bulk resistance can more significantly influence the performance of inverted PSCs with sputtered ZnO layer. The vanishment of negative capacitive behavior of inverted PSCs with ILCNs modified ZnO layer indicated ILCNs can greatly decrease the contact barrier of ZnO/P3HT:PCBM interface.

Keywords: Polymer; Solar cell; ZnO

Citation: Feng Zhu, Xiaohong Chen, Zhe Lu, Jiaxiang Yang, Sumei Huang and Zhuo Sun, "Efficiency Enhancement of Inverted Polymer Solar Cells Using Ionic Liquid-functionalized Carbon Nanoparticles-modified ZnO as Electron Selective Layer", *Nano-Micro Lett.* 6(1), 24-29 (2014). <http://dx.doi.org/10.5101/nml.v6i1.p24-29>

Introduction

Polymer solar cells (PSCs) have been attracting considerable attention due to its mechanical flexibility, low cost fabrication and light weight [1,2]. PSCs have been quickly developed in the past several years. Power conversion efficiency (PCE) of more than 6% ~10% has been reported for both conventional and inverted PSC structures [3-6]. In conventional PSCs, the photoactive layer is sandwiched with poly(3,4-

ethylenedioxythiophene)/poly(styrenesulfonate) (PEDOT:PSS) and low work function metal (such as Al and Ca/Ag) as an anode contact layer and cathode, respectively. However, PEDOT:PSS layer is detrimental to ITO anode due to its acidic property, resulting in reducing device lifetime [7,8]. The inverted PSCs can effectively overcome shortage of traditional PSCs by selection and optimization of n-type and p-type materials as electron and hole selective layers, respectively.

¹Engineering Research Center for Nanophotonics and Advanced Instrument, Ministry of Education, and Department of Physics, East China Normal University, Shanghai 200062, China

²Department of Chemistry, Anhui University, Hefei, Anhui Province 230039, China

*Corresponding author. E-mail: xhchen@phy.ecnu.edu.cn

ZnO as an electron selective material has received much attention due to its high electron mobility and good optical transparency. However, the electrical properties of ZnO films are strongly depended on its synthetic method and fabrication process. The sol-gel derived ZnO layer need usually be annealed under high temperature to decompose of zinc acetate precursor and increase the carrier mobility, which inhibits its application in plastic substrates [9]. Recently, PSCs based on solution-processed ZnO nanoparticles have been developed without high temperature treatment [10,11]. However, synthetic ZnO nanoparticle size and thickness of ZnO electron selective layer need precisely be controlled to gain high performance of PSCs. Magnetron sputtering deposition technique is mature and used widely in industry due to easily precisely controlling film composition and thickness, strong operability and batch production. Recently, ZnO electron selective layers in PSCs have been studied with magnetron sputtering deposition [12,13]. Developing ZnO as electron selective layer using magnetron sputtering deposition is compatible with present commercial tin-doped indium oxide (ITO) and aluminium-doped zinc oxide (AZO) transparent conducting films, which can simplify procedure and control cost of PSCs [14,15]. However, the performance of PSCs is closely related to ZnO sputtering condition, thickness and annealing temperature. In this paper, ZnO electron selective layer was deposited onto ITO-coated glass by magnetron sputtering technique without adding substrate temperature. Ionic liquid-functionalized carbon nanoparticles (ILCNs) film was further deposited onto ZnO surface to modify interface potential between ZnO and photoactive layers. The range of sputtering condition and thickness of ZnO layer were significantly extended for PSCs after modified with ILCNs film.

Experimental procedure

ZnO electron selective layer was deposited onto ITO coated glass substrate by magnetron sputtering without substrate temperature, using a ZnO target of 99.99% purity. All samples were deposited with RF power 50 W and sputtering pressure 0.3 Pa under a base pressure of 2×10^{-3} Pa. The total sputtering Ar gas flow was 20 sccm. ILCNs were synthesized by the electrochemical exfoliation of graphite electrode in 1-butyl-3-methylimidazolium tetrafluoroborate ([bmim][BF₄]) and water mixture (40:60) [16]. The ILCNs synthetic process and its properties have been reported [16-18]. The size of ILCNs is below 4 nm by transmission electron microscopy images. The ILCNs film was spin-coated onto ZnO surface with estimated thickness of 1-3 nm. The solution of P3HT:PCBM (1:0.8) in dichlorobenzene was spin-coated onto electron selective

layer to form 200 nm thick film. Finally, the 14 nm MoO₃ and 150 nm Al electrode were thermally evaporated onto P3HT:PCBM blend film to form an anode under a background pressure of 2.5×10^{-6} Torr. The active area of device was 0.1 cm². Current-voltage (*C* – *V*) curves were measured under AM1.5G illumination intensity of 100 mW/cm² using a Newport solar simulator system.

Results and discussion

The light absorption range of P3HT:PCBM film is primarily from 400 nm to 600 nm. The optical transmittance spectra of different thick ZnO film on ITO coated glass substrate are shown in Fig. 1. The average optical transmittance (79.2%) of ZnO/ITO coated glass in the range from 400 nm to 600 nm is below 3.3% than that of pure ITO coated glass (82.5%). Accordingly, about 80.7% average transmittance of ILCNs-modified ZnO surface means that ILCNs films have good transparency, as previous report of ILCNs modified ITO glass [17]. Furthermore, only 1.5% transmittance difference indicates that the optical absorption difference of PSCs with ZnO electron selective layer can be excluded to explain the performance of PSCs.

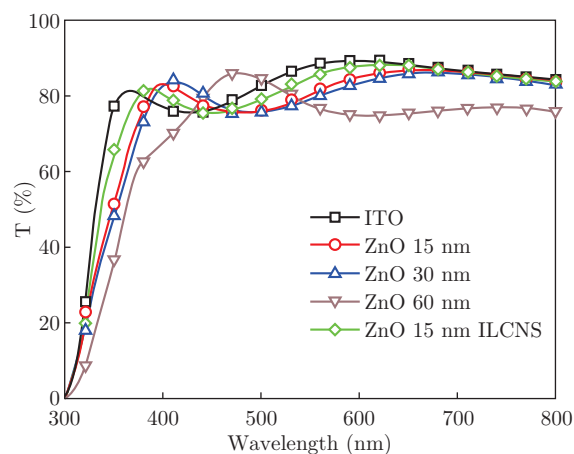


Fig. 1 Optical transmittance spectra of different thickness ZnO film on ITO coated glass substrate.

The current density-voltage (*J* – *V*) curves of PSCs with/without ILCNs modified on different thickness ZnO layer are shown in Fig. 2. Table 1 summarizes the relevant average parameters of PSCs. The PCE was reduced from 2.7% to 2.2%, open-circuit voltage (*V*_{oc}) from 0.49 V to 0.45 V, and fill factor (FF) from 0.48 to 0.42, as ZnO thickness was increased from 15 nm to 60 nm. After ZnO surface was modified with ILCNs, the performance difference induced by ZnO thickness was significantly reduced and *J* – *V* curves were almost overlapped in large part interval. The performance of PSCs with ILCNs modified ZnO surface can be greatly improved compared to PSCs without ILCNs. The *V*_{oc},

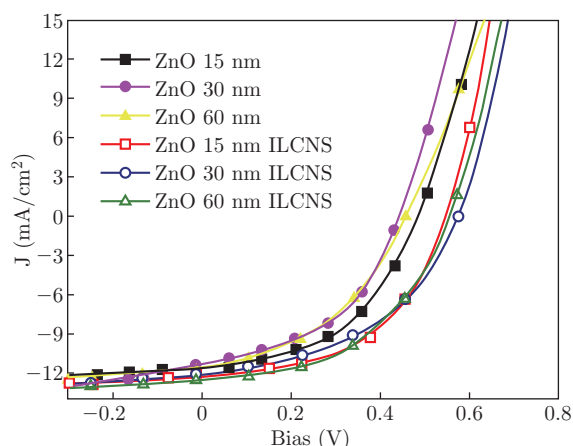


Fig. 2 The J - V characteristics of different types of representative PSCs.

Table 1 Average parameters of inverted PSCs based on ZnO layers thickness varied and modified with/without ILCNs

ITO/(buffer layer)	V_{oc} (V)	J_{sc} (mA/cm ²)	FF	PCE (%)	R_s (Ω /cm ²)
ZnO (15 nm)	0.49	11.5	0.48	2.7	2.4
ZnO (30 nm)	0.45	11.4	0.46	2.4	3.5
ZnO (60 nm)	0.45	11.6	0.42	2.2	10.5
ZnO (15 nm)-ILCNS	0.55	12.2	0.52	3.5	1.3
ZnO (30 nm)-ILCNS	0.56	12.0	0.50	3.4	2.3
ZnO (60 nm)-ILCNS	0.56	12.5	0.48	3.4	2.4

FF and PCE of the best performance PSCs with ILCNs modified 15 nm ZnO layer are 0.55 V, 0.52 and 3.5%, respectively. The V_{oc} , FF and PCE of PSCs with ILCNs modified 60 nm thick ZnO buffer layer are obviously larger than that of PSCs with only 60 nm ZnO layer. The average PCE of PSCs with ILCNs modified 60 nm ZnO layer is almost close to that of PSCs with 15 nm ZnO layer or traditional PSCs. Its increasing range was greater than that of 15 nm ZnO layer. The improving PCE of PSCs with ILCNs modified 60 nm ZnO layer is attributed to reducing the contact resistance [19] and obviously reverse saturation current, as shown in Fig. 3. The increasing leakage current of PSCs with 60 nm ZnO layer can result in deteriorated FF (0.4) and V_{oc} (0.45 V). Through modified with ILCNs, the reverse saturation current was obviously decreased and rectifying property was improved. This means that the electron recombination is reduced and the electron accumulation phenomenon is weakened at ZnO/P3HT interface by ILCNs modified ZnO layer, which is helpful to improving V_{oc} and photocurrent of PSCs. The slightly decreasing serial resistance of PSCs based on 15 nm and 30 nm ZnO layer modified with ILCNs compared to without ILCNs indicates that interface contact properties of ZnO/P3HT:PCBM after modified ILCNs are improved for thin thickness of ZnO layer. Its se-

ries resistance (R_s) was decreased from 10.5 Ω /cm² to 2.4 Ω /cm² after ILCNs modified with 60 nm thick ZnO layer, further suggesting that the deteriorated FF and V_{oc} are primarily ascribed to interface properties of ZnO layer.

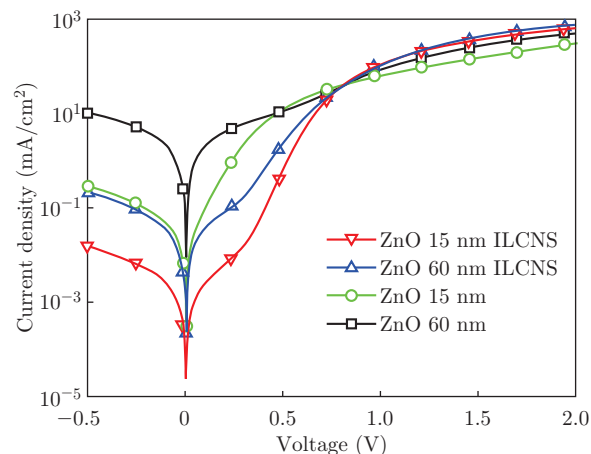


Fig. 3 The dark J - V curves of PSCs.

Impedance spectroscopy is a powerful technique to derive insights into the interfacial properties and the charge carrier dynamics of PSCs [20]. The different interface barrier between ZnO layer and the active layer is expected to affect carrier accumulation and transportation, resulting in differences in the device capacitance. Figure 4 shows the impedance spectra of PSCs with 30 nm ZnO layer modified with/without ILCNs in the dark. The impedance plots of Fig. 4(a) exhibits an arc in the fourth quadrant at the low frequency range at the voltage of 0.5 V and 0.6 V, indicating the negative capacitance exists in PSCs without ILCNs modified ZnO layer. After modified with ILCNs, the $-\text{Im}(Z)$ values are always positive at any voltages and frequencies, as shown in Fig. 4(b). Garcia-Belmonte et al reported that the negative capacitive behavior would be appeared due to the Schottky contact at P3HT:PCBM/Al [20]. The massive electrons were accumulated in the vicinity of cathode due to high interface barrier under moderate forward bias, which can result in the negative capacitive behavior. The negative capacitive behavior of P3HT:PCBM/Al disappeared after ILCNs modified with Al cathode was further reported by Chen et al. [18], indicating low interface barrier or ohmic contacts at the cathode. Similarly, the negative capacitive behavior in PSCs of ZnO layer without ILCNs may be attributed to the electron accumulation at the interface of ZnO/P3HT:PCBM due to high contact barrier. Subsequent experiments show that with increasing ZnO sputtering thickness, negative capacitive behavior becomes more obvious and the radius of circle in fourth quadrant become larger. The ILCNs modified 60 nm layer can still eliminate negative capacitive phenomenon.

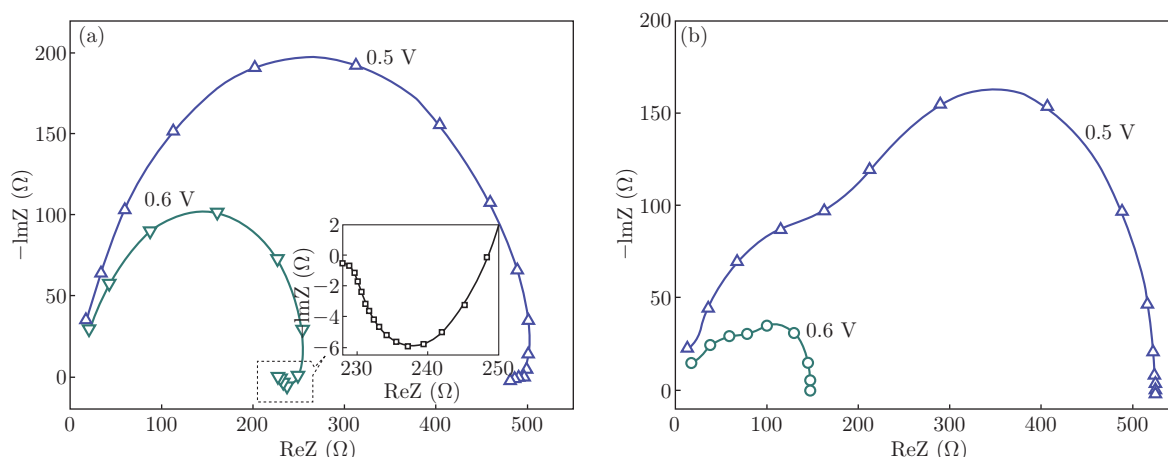


Fig. 4 Bias dependence of Cole-Cole plots of inverted PSCs with 30 nm thick ZnO layer (a), and 30 nm ZnO layer modified with ILCNs (b).

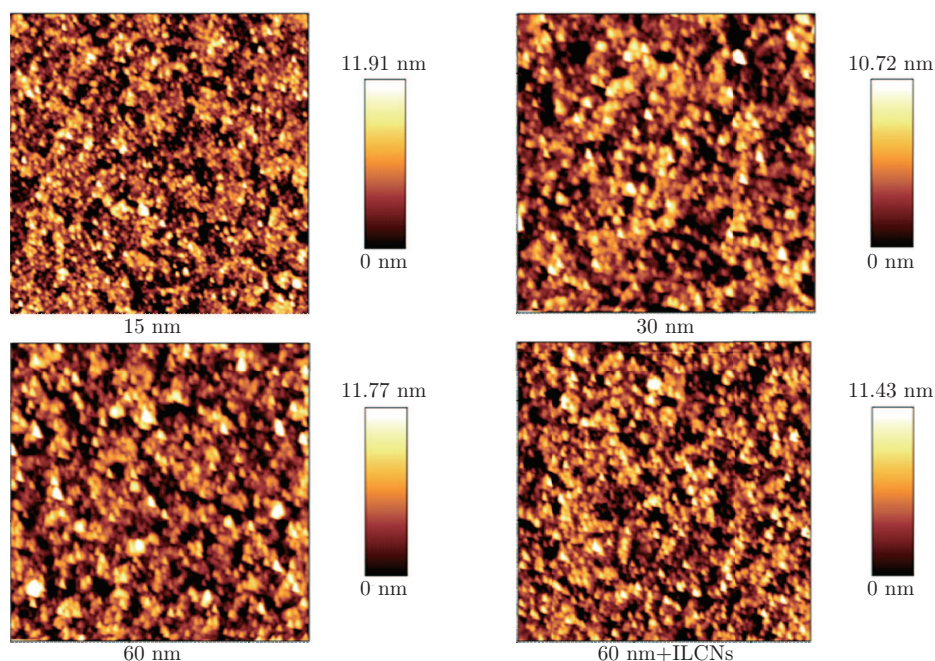


Fig. 5 Surface morphology images of ZnO films with 15 nm, 30 nm, 60 nm and ILCNs modified 60 nm thickness. The size of AFM images is $5 \times 5 \mu\text{m}^2$.

Although further experiments showed that optimized sputtering condition, for example adding O_2 gas flow at certain ratio can also eliminate the negative capacitive behavior at 30 nm layer, not applicable for 60 nm. This indicates that the employment of ILCNs can enlarge the selective layer thickness and reduced the preparation requirement. This is important for industry to increase product rate and decrease product cost.

To further explain the effect of ILCNs modified ZnO layer on decreasing contact barrier, the surface morphologies were measured by atomic force microscopy (AFM). Figure 5 shows AFM surface morphologies of ZnO films. The root-mean-square (RMS) roughness of 15 nm, 30 nm and 60 nm ZnO films are 2.12 nm, 2.67 nm and 4.45 nm, respectively. After ILCNs modified 60

nm ZnO film, RMS roughness of ZnO films is decreased from 4.45 nm to 1.89 nm. The rougher surface can result in deteriorated films and easily form pinholes in the photoactive layer. The higher reverse saturation current for PSCs with 60 nm ZnO layer compared to thinner ZnO layer and ILCNs modified ZnO layer is consistent with this observation. In addition, the sp^2 bonded aromatic structure of carbon nano-particles can provide low tunneling barrier height at the interfacial contact. The ions of ILCNs can form electric double layer at the interface between the active layer and ILCNs, which is helpful to reducing electron injection/extraction barrier [18]. The greatly lower work function of ILCNs modified ITO (3.8 eV) compared to bare ITO (4.4 eV) reported further supports this prediction [17].

Conclusions

In summary, the ILCNs modified ZnO layer was successfully applied to improve the ZnO/P3HT contact quality and gained good PSCs performance. The average PCE of PSCs with ILCNs modified ZnO layer thickness ranging from 15 nm to 60 nm is almost comparable to that of traditional PSCs with PEDOT:PSS anode buffer layer. Through adding ILCNs, the selective layer ZnO thickness was enlarged and reduced the interface contact barrier. The PCE of inverted PSCs based on ZnO electron selective layer deposited with magnetron sputtering method is more sensitive to the surface characteristic of ZnO films than ZnO layer thickness. ILCNs can avoid the impact on device performance caused by increasing sputtered ZnO thickness. In the mean time, the good performance of inverted PSCs achieved by ILCNs modified different thick ZnO layer also indicates that magnetron sputtering deposition is an easily controlling method to fabricate ZnO layer as a good electron selective layer.

Acknowledgements

This work was supported by National Natural Science Foundation of China (grant Nos. 61275038, 11274119), Natural Science Foundation of Shanghai Science and Technology Commission (grant No. 11ZR1411300), Pujiang Talent Program of Shanghai Science and Technology Commission (grant No. 11PJ1402700), Doctoral Fund of Ministry of Education of China (grant No. 20110076120017) and SRF for ROCS, SEM.

References

- [1] F. C. Krebs, J. Fyenbo and M. Jørgensen, "Product integration of compact roll-to-roll processed polymer solar cell modules: methods and manufacture using flexographic printing, slot-die coating and rotary screen printing", *J. Mater. Chem.* 20(41), 8994-9001 (2010). <http://dx.doi.org/10.1039/C0JM01178A>
- [2] N. Espinosa, M. Hösel, D. Angmo and F. C. Krebs, "Solar cells with one-day energy payback for the factories of the future", *Energy Environ. Sci.* 5(1), 5117-5132 (2012). <http://dx.doi.org/10.1039/C1EE02728J>
- [3] Z. He, C. Zhong, S. Su, M. Xu, H. Wu and Y. Cao, "Enhanced power-conversion efficiency in polymer solar cells using an inverted device structure", *Nature Photonics* 6(9), 591-595 (2012). <http://dx.doi.org/10.1038/nphoton.2012.190>
- [4] T. Y. Chu, J. Lu, S. Beaupré, Y. Zhang, J. R. Pouliot, S. Wakim, J. Zhou, M. Leclerc, Z. Li and J. Ding, "Bulk heterojunction solar cells using thieno[3,4-c]pyrrole-4,6-dione and dithieno[3,2-b:2',3'-d] silole copolymer with a power conversion efficiency of 7.3%", *J. Am. Chem. Soc.* 133(12), 4250-4253 (2011). <http://dx.doi.org/10.1021/ja200314m>
- [5] J. You, L. Dou, K. Yoshimura, T. Kato, K. Ohya, T. Moriarty, K. Emery, C.-C. Chen, J. Gao, G. Li and Y. Yang, "A polymer tandem solar cell with 10.6% power conversion efficiency", *Nat. Commun.* 4, 1446 (2013). <http://dx.doi.org/10.1038/ncomms2411>
- [6] Z. He, C. Zhong, X. Huang, W. Y. Wong, H. Wu, L. Chen, S. Su and Y. Cao, "Simultaneous enhancement of open-circuit voltage, short-circuit current density, and fill factor in polymer solar cells", *Adv. Mater.* 23(40), 4636-4643 (2011). <http://dx.doi.org/10.1002/adma.201103006>
- [7] K. Wong, H. Yip, Y. Luo, K. Wong, W. Lau, K. Low, H. Chow, Z. Gao, W. Yeung and C. Chang, "Blocking reactions between indium-tin oxide and poly (3,4-ethylene dioxythiophene):poly(styrene sulphonate) with a self-assembly monolayer", *Appl. Phys. Lett.* 80(15), 2788-2790 (2002). <http://dx.doi.org/10.1063/1.1469220>
- [8] T. Nguyen and S. De Vos, "An investigation into the effect of chemical and thermal treatments on the structural changes of poly(3,4-ethylenedioxythiophene)/polystyrenesulfonate and consequences on its use on indium tin oxide substrates", *Appl. Surf. Sci.* 221(1), 330-339 (2004). [http://dx.doi.org/10.1016/S0169-4332\(03\)00952-8](http://dx.doi.org/10.1016/S0169-4332(03)00952-8)
- [9] A. Kyaw, X. Sun, C. Jiang, G. Lo, D. Zhao and D. Kwong, "An inverted organic solar cell employing a sol-gel derived ZnO electron selective layer and thermal evaporated MoO₃ hole selective layer", *Appl. Phys. Lett.* 93(22), 221107-221107 (2008). <http://dx.doi.org/10.1063/1.3039076>
- [10] T. Chang, Z. Li, G. Yun, Y. Jia and H. Yang, "Enhanced photocatalytic activity of ZnO/CuO nanocomposites synthesized by hydrothermal method", *Nano-Micro Lett.* 5(3), 163-168 (2013). <http://dx.doi.org/10.5101/nml.v5i3.p163-168>
- [11] S. K. Hau, H.-L. Yip, N. S. Baek, J. Zou, K. O'Malley and A. K.-Y. Jen, "Air-stable inverted flexible polymer solar cells using zinc oxide nanoparticles as an electron selective layer", *Appl. Phys. Lett.* 92, 253301 (2008). <http://dx.doi.org/10.1063/1.2945281>
- [12] Y. Jouane, S. Colis, G. Schmerber, P. Kern, A. Dini, T. Heiser and Y.-A. Chapuis, "Room temperature ZnO growth by rf magnetron sputtering on top of photoactive P3HT: PCBM for organic solar cells", *J. Mater. Chem.* 21(6), 1953-1958 (2011). <http://dx.doi.org/10.1039/C0JM02354J>
- [13] J. Hu, Z. Wu, H. Wei, T. Song and B. Sun, "Effects of ZnO fabricating process on the performance of inverted organic solar cells", *Org. Electron.* 13(7), 1171-1177 (2012). <http://dx.doi.org/10.1016/j.orgel.2012.03.021>
- [14] J.-A. Jeong and H.-K. Kim, "Low resistance and highly transparent ITO-Ag-ITO multilayer electrode using surface plasmon resonance of Ag layer for bulk-heterojunction organic solar cells", *Sol. Energy Mater.*

- Sol. Cells 93(10), 1801-1809 (2009). <http://dx.doi.org/10.1016/j.solmat.2009.06.014>
- [15] C. Guillén and J. Herrero, "TCO/metal/TCO structures for energy and flexible electronics", *Thin Solid Films* 520(1), 1-17 (2011). <http://dx.doi.org/10.1016/j.tsf.2011.06.091>
- [16] J. Lu, J. Yang, J. Wang, A. Lim, S. Wang and K. P. Loh, "One-Pot Synthesis of Fluorescent Carbon Nanoribbons, Nanoparticles, and Graphene by the Exfoliation of Graphite in Ionic Liquids", *ACS nano* 3(8), 2367-2375 (2009). <http://dx.doi.org/10.1021/nn900546b>
- [17] X. Chen, J. Yang, L. Y. X. C. Haley, J. Lu, F. Zhu and K. P. Loh, "Towards high efficiency solution processable inverted bulk heterojunction polymer solar cells using modified indium tin oxide cathode", *Org. Electron.* 11(12), 1942-1946 (2010). <http://dx.doi.org/10.1016/j.orgel.2010.09.011>
- [18] X. Chen, J. Yang, J. Lu, K. K. Manga, K. P. Loh and F. Zhu, "Ionic liquid-functionalized carbon nanoparticles-modified cathode for efficiency enhancement in polymer solar cells", *Appl. Phys. Lett.* 95(13), 133305 (2009). <http://dx.doi.org/10.1063/1.3237161>
- [19] A. Tada, Y. Geng, M. Nakamura, Q. Wei, K. Hashimoto and K. Tajima, "Interfacial modification of organic photovoltaic devices by molecular self-organization", *Phys. Chem. Chem. Phys.* 14(11), 3713-3724 (2012). <http://dx.doi.org/10.1039/C2CP40198C>
- [20] G. Garcia-Belmonte, A. Munar, E. M. Barea, J. Bisquert, I. Ugarte and R. Pacios, "Charge carrier mobility and lifetime of organic bulk heterojunctions analyzed by impedance spectroscopy", *Org. Electron.* 9(5), 847-851 (2008). <http://dx.doi.org/10.1016/j.orgel.2008.06.007>